Physically-Constrained Diffeomorphic Demons for the Estimation of 3D Myocardium Strain from Cine-MRI

Tommaso Mansi[1], Jean-Marc Peyrat[1], Maxime Sermesant[1], Hervé Delingette[1], Julie Blanc[2], Younes Boudjemline[2], and Nicholas Ayache[1]

[1] INRIA-Méditerranée, Asclepios Project, Sophia Antipolis, France
[2] Assistance Publique Hôpitaux de Paris, Necker-Enfants Malades, Paris, France

Abstract. Analysing heart motion provides crucial insights on the condition of the cardiac function. Tagged-MRI and 2D-strain ultrasound enable quantitative assessment of the myocardium strain. But estimating 3D myocardium strain from cine-MRI remains attractive: cine-MRI is widely available and it yields detailed 3D+t anatomical images. This paper presents an image-based method to estimate myocardium strain from clinical short-axis cine-MRI. To recover non-apparent cardiac motions, we improve the diffeomorphic demons, a non-linear registration algorithm, by adding two physical constraints. First, myocardium near-incompressibility is ensured by constraining the deformations to be divergence free. Second, myocardium elasticity is modelled using smooth vector filters. The proposed physically-constrained demons are compared with the diffeomorphic demons and evaluated in a healthy subject against tagged MRI. The method is also tested on a patient with congenital pulmonary valve regurgitations and compared with 2D-strain measurements. In both cases, obtained results correlate well with ground truth. This method may become a useful tool for cardiac function evaluation.

1 Introduction

Analysing heart motion provides crucial insights on the condition and efficiency of the cardiac function. Myocardium strain can now be quantitatively assessed through tagged-MRI or ultrasound modalities such as 2D speckle tracking (also known as 2D-strain). Nevertheless, despite of its accuracy, tagged-MRI is still experimental [1] and while 2D-strain becomes available in clinical environment, it only provides partial evaluation of the myocardium [2]. Estimating the myocardium strain from clinical gated cine-MRI constitutes an attractive alternative. Cine-MRI is widely available and yields detailed 3D anatomical images of the beating heart with constant image quality through time. However, estimating strain from these images may result inaccurate since only the apparent motion can be extracted and slice thickness is usually large. Prior knowledge about cardiac dynamics is thus required.

N. Ayache, H. Delingette, and M. Sermesant (Eds.): FIMH 2009, LNCS 5528, pp. 201–210, 2009.

Various methods have been proposed to estimate myocardium deformation from cine-MRI [3,4,5,6,7]. Some approaches drive an image registration algorithm with biomechanical finite-element models that simulate the myocardium passive properties [3,4]. These methods successfully estimate left ventricle myocardium strain. Nonetheless, they rely on specific biomechanical parameters that are difficult to determine for a given patient. Besides, such models may not apply anymore in diseases. Purely image-driven methods have thus been proposed [5,6,7]. In [5], the authors use a B-spline Free-Form Deformation (FFD) algorithm regularised using myocardium contours that are manually delineated on all time frames. The results are consistent with tagged MRI but requiring manual contours for all time frames may hamper using this approach in clinical settings. In [6], Bistoquet *et al.* present an FFD-like algorithm that ensures myocardium near-incompressibility [8]. The similarity criterion is penalised when the Jacobian of the deformation is significantly different from 1 and the dense deformation field is estimated by using divergence-free radial basis functions. However, myocardium is tracked at the nodes of the epicardium and endocardia surfaces only, the inner deformations being interpolated from the surfaces without considering possible textural hints. In [7], the authors estimate the cardiac motion using a spatio-temporal model based on FFD and Kalman filters, under the assumption of periodic motion. However, the proposed approach does not take guarantee myocardium biomechanical properties and it has been validated on 2D+t images only.

This paper presents an image-based method to estimate myocardium strain from clinical short-axis cine-MRI. Our approach relies on diffeomorphic demons [9], an efficient non-linear registration algorithm. Diffeomorphic non-linear registration [9,10,11] aims at finding a smooth, invertible, one-to-one mapping between two images, which is suited for cardiac motion analysis. Because diffeomorphic demons rely on image data exclusively, we introduce in the algorithm two physical constraints to recover plausible non-apparent cardiac motions: *i)* myocardium near-incompressibility [8] and *ii)* elasticity. Integrating incompressibility in non-linear registration algorithms has been widely studied for contrast-enhanced image registration [12,13,14]. Incompressibility can be modelled through the hard constraint Jacobian determinant of the deformation field equals 1 [12,13], or through the divergence-free approximation [6,14]. In our approach, near-incompressibility is obtained by projecting the velocity and deformation fields onto the space of divergence-free vector fields. The second physical constraint we consider is myocardium elasticity, modelled with an elastic-like regularisation. Although myocardium tissue is found visco-elastic, it can be reasonably modelled as elastic when it is analysed at the heart beat time-scale [8]. In this way, our approach is purely image-based, it evaluates the motion everywhere in the images, it does not need any mesh model and it requires very few image-based parameters. The Lagrangian finite strain tensor is finally calculated from the recovered deformation fields. The method is evaluated on a healthy subject, against tagged MRI, and on a patient suffering from congenital pulmonary valve regurgitations, against 2D-strain ultrasound.

2 Methods

2.1 Non-linear Image Registration Using Diffeomorphic Demons (DD) Algorithm

Non-linear image registration aims at providing a transformation $\phi(\mathbf{x}) = \mathbf{x} + \mathbf{u}(\mathbf{x})$, where $\mathbf{u}(\mathbf{x})$ is the displacement vector field, that aligns a template image $T(\mathbf{x})$ with a reference image $R(\mathbf{x})$. The underlying principle lies in minimising an energy $\mathcal{E}(\phi)$ that comprises a similarity criterion $\mathcal{D}(T, R, \phi)$ and a regulariser $\mathcal{R}(\phi)$ ensuring smooth transformations and integrating prior knowledge.

Diffeomorphic demons (DD) algorithm [9] minimises $\mathcal{E}(\phi)$ iteratively through two decoupled steps. A correspondence field $\mathbf{c}$ that matches the points between the two images, with a controlled uncertainty parametrised by σ_x^2, is introduced in the energy: $\mathcal{E}(\mathbf{c}, \mathbf{u}) = 1/\sigma_i^2 \ \|R - T \circ \mathbf{c}\|^2 \ + \ 1/\sigma_x^2 \ \|\mathbf{u} - \mathbf{c}\|^2 \ + \ 1/\sigma_T^2 \ \|\nabla \mathbf{u}\|^2$. In this equation, σ_i^2 is a parameter related to the noise in the images and σ_T^2 compromises between the image data term and the regularisation.

First, the correspondence field $\mathbf{c}$ is updated using the diffeomorphic update rule $\mathbf{c} \leftarrow \mathbf{u} \circ \exp(\mathbf{v})$. $\exp(\mathbf{v})$ is the exponential operator defined in the Log-Euclidian framework and $\mathbf{v}$ is the smooth stationary *velocity* field that results from the minimisation of the correspondence energy:

$$\mathcal{E}_{corr}(\mathbf{v}) = \frac{1}{\sigma_i^2}\|R - T \circ \mathbf{u} \circ \exp(\mathbf{v})\|^2 + \frac{1}{\sigma_x^2} \ \|\mathbf{u} - \mathbf{u} \circ \exp(\mathbf{v})\|^2 \qquad (1)$$

Derivating $\mathcal{E}_{corr}$ yields $\mathbf{v} = -(R - T \circ (\mathrm{Id} + \mathbf{u}))/(\|J\|^2 + \sigma_i^2/\sigma_x^2) \ J$, with $J = (\nabla R + \nabla(T \circ (\mathrm{Id} + \mathbf{u})))/2$ and $\sigma_i = |R - T \circ (\mathrm{Id} + \mathbf{c})|$ (see [9] for further details).

Second, the displacement $\mathbf{u}$ that satisfies the regulariser $\mathcal{R}(\mathbf{u})$, knowing the new correspondence field $\mathbf{c}$, is computed. The second part of the demons energy $\mathcal{E}(\mathbf{c}, \mathbf{u})$, $\mathcal{E}_{reg}(\mathbf{c}, \mathbf{u}) = 1/\sigma_x^2 \ \|\mathbf{u} - \mathbf{c}\|^2 + 1/\sigma_T^2 \|\nabla \mathbf{u}\|^2$, is minimised with respect to $\mathbf{u}$, which amounts to convoluting $\mathbf{c} = \mathbf{u} \ \circ \ \exp(\mathbf{v})$ with a Gaussian kernel.

2.2 Adding Physical Constraints to the Diffeomorphic Demons

Diffeomorphic demons (DD) algorithm is purely driven by image intensities. Therefore, it can hardly recover longitudinal shortening and circumferential twisting, which are poorly apparent in short-axis cine-MRI. To better estimate these displacements, we improve the algorithm by adding two constraints related to the myocardium tissue properties: near-incompressibility and elasticity.

Incompressibility Constraint. Contrary to [13], the incompressibility constraint is decoupled from the energy minimisation to take advantage of the two-step minimisation process offered by the demons. Since DD relies on velocity fields, fluid-dynamics laws are used to model incompressibility [14]. However, slight volume drifts may remain as the Gaussian regularisation does not preserve incompressibility. Positions are hence corrected at the end of the demons loop to further reduce volume variations.

Velocity Correction: Myocardium incompressibility can be interpreted as conservation of myocardium mass throughout the cardiac cycle [8]. Therefore, the mass continuity equation $\partial\rho/\partial t + \mathrm{div}(\rho\mathbf{v}) = 0$ applies, where ρ is the mass density, $\mathbf{v}$ is the velocity and t is the time. Assuming ρ constant and uniform, the conservation of mass becomes conservation of volume and writes as $\mathrm{div}(\mathbf{v}) = 0$.

Consequently, the incompressibility property is integrated in the DD by constraining the search space of the velocity fields $\mathbf{v}$ to the divergence-free vector space. Given the velocity field $\mathbf{v}$ computed by Equation (1), we solve the Lagrangian problem [15]:

$$\min_{\hat{\mathbf{v}} \in \{\mathbf{f} \in L^2(\Omega) \mid \mathrm{div}\ \mathbf{f} = 0\}} \max_{p \in \mathrm{H}_0^1} \left(\frac{1}{2}\|\mathbf{v} - \hat{\mathbf{v}}\|^2 + \int_\Omega p\ \mathrm{div}\ \hat{\mathbf{v}} \right) \tag{2}$$

In this equation, Ω is an open subset of $\mathbb{R}^3$ (the image space), $\mathrm{H}_0^1(\Omega)$ is the Sobolev space associated to Ω and p is the Lagrange multiplier related to the divergence-free constraint. Derivating Equation (2) gives the optimal condition:

$$\hat{\mathbf{v}} = \mathbf{v} - \mathrm{grad}\ p \tag{3}$$

under the constraint $\mathrm{div}\ \hat{\mathbf{v}} = 0$. Equation (3) is the closed-form expression of the divergence-free projector $\Pi(\mathbf{v}) = \mathbf{v} - \mathrm{grad}\ p$, where p is obtained by solving the Poisson equation $\triangle p = \mathrm{div}(\mathbf{v})$ under 0-Dirichlet boundary conditions [15].

Position Correction: Because the Gaussian regularisation may alter the obtained incompressibility, we perform a second adjustment to correct the remaining volume drifts after deformation.

For each point $\mathbf{x}$ of the image space, the Jacobian determinant $J(\mathbf{x}) = \det(\mathrm{Id} + \nabla\mathbf{u}(\mathbf{x}))$ relates to the local volume change due to the transformation $\phi(\mathbf{x}) = \mathbf{x} + \mathbf{u}(\mathbf{x})$. Hence, the volume is locally preserved if the non-linear constraint $J(\mathbf{x}) = 1$ is satisfied. However, since myocardium is *nearly* incompressible (5% of volume variation is usually observed [6,8]) and the displacements provided by the DD are smooth and derive from divergence-free velocities, the first-order approximation of $J(\mathbf{x}) = 1$, i.e. $\mathrm{div}(\mathbf{u}) = 0$, can be used to correct the remaining volume drifts. As a result, the positions are corrected like the velocities. At each iteration of the demons algorithm, the displacement field $\mathbf{u}$ is made divergence-free by using the above-mentioned projector Π (Equation (3)). It is worth stressing that the displacements are projected to reduce remaining volume drifts, whereas the velocities are projected as a result of the mass-conservation law.

Elastic-Like Regularisation. Myocardium is commonly assumed to be visco-elastic. However, at the time-scale of the heart beat, one can reasonably approximate the visco-elasticity property by elasticity [8]. In our approach, elasticity is modelled as regularisation. We substitute the diffusion-like regularisation, which is unable to model elastic deformations, by an elastic regulariser. Linear elastic regularisers have been widely studied in the past [16]. Yet, they are suitable for small displacements only and can present discontinuities in the derivatives of

the resulting deformations, which is not desirable for our application. To overcome these limitations, we regularise the deformation field using an infinite-order isotropic differential quadratic form [17]. Such regulariser behaves like elastic filters, while ensuring smooth deformations. Minimising $\mathcal{E}_{reg}(\mathbf{c}, \mathbf{u})$ with this regulariser amounts to convoluting the deformation field $\mathbf{u}$ by the 3D isotropic separable filter:

$$G_{\sigma,\kappa}(\mathbf{u}) = \frac{1}{(\sigma\sqrt{2\pi})^3(1+\kappa)} \left(\mathrm{Id} + \frac{\kappa}{\sigma^2}\mathbf{u}\mathbf{u}^T\right) \exp\left(\frac{\mathbf{u}^T\mathbf{u}}{2\sigma^2}\right) \tag{4}$$

which can be performed very efficiently by using recursive Gaussian filter [17]. In Equation (4), σ is the standard deviation of the Gaussian function and κ is a parameter that acts as a Poisson ratio coefficient. The higher is κ, the stiffer is the deformation.

Final Algorithm. Bellow we summarise the steps of the physically-constrained demons. Steps with a star (*) relates to the new physical constraints.

Physically-Constrained Demons (PCD) Algorithm

- Choose an initial spatial transformation $\phi(\mathbf{x}) = \mathbf{x} + \mathbf{u}(\mathbf{x})$
- Iterate until $\mathcal{D}(R, T; \mathbf{u})$ stops decreasing
  1. Given the current deformation $\mathbf{u}$, compute the update velocity field $\mathbf{v}$ by minimising $\mathcal{E}_{corr}(\mathbf{v})$ (Equation (1)).
  2. Fluid-like regularisation: $\mathbf{v} \leftarrow K_{fluid} \star \mathbf{v}$. K_{fluid} is typically a Gaussian kernel with standard deviation σ_{fluid}.
  3. (*) Correct the velocity to be divergence-free: $\mathbf{v} \leftarrow \Pi(\mathbf{v})$.
  4. Update the correspondence field: $\mathbf{c} \leftarrow \mathbf{u} \circ \exp(\mathbf{v})$
  5. (*) Elastic-like regularisation: $\mathbf{u} \leftarrow G_{\sigma,\kappa} \star \mathbf{c}$ (Equation (4))
  6. (*) Correct the deformation to be divergence-free: $\mathbf{u} \leftarrow \Pi(\mathbf{u})$.

About the algorithm parameters. PCD algorithm is controlled by four parameters: the maximum step length [9], σ_{fluid}, σ and κ. In all our experiments, we have used standard values according to previous experiments [9,17]: the maximum step length is 1, σ_{fluid} is 0.5, σ is 2.0 and κ is 0.5.

2.3 Estimating Strain from Cine-MRI

Strain is estimated from cine MRI by tracking the myocardium throughout the cardiac sequence. Let I_0 be the end-diastole time frame. Since DD algorithm is expressed in the Eulerian frame [16] and strain is computed in the Lagrangian frame, the tracking must be performed backwards: the strain between the images I_0 and $I_{n>0}$ is computed from the deformation obtained by registering $I_{n>0}$ to I_0. A recursive strategy is employed to take advantage of the frame-by-frame registration accuracy and to reduce tracking errors due to the changing appearance of the trabecula, papillary muscles and neighbouring

organs. Having the spatial transformation $\phi_{I_{n-1} \to I_0}$, we first compute $\phi_{I_n \to I_{n-1}}$ and then we estimate the transformation $\phi_{I_n \to I_0}$ by taking as initialisation the composed transformation $\phi_{I_n \to I_{n-1}} \circ \phi_{I_{n-1} \to I_0}$. Finally, Lagrangian finite strain tensor $\mathrm{E} = 1/2\ (\nabla \mathbf{u} + \nabla \mathbf{u}^T + \nabla \mathbf{u}^T \nabla \mathbf{u})$ is computed from the recovered deformation $\phi(\mathbf{x}) = \mathbf{x} + \mathbf{u}(\mathbf{x})$. Radial, circumferential and longitudinal strains are estimated in the heart prolate coordinate system [18].

3 Experiments and Results

The method is tested on two subjects: a healthy adult and a young patient suffering from congenital pulmonary valve regurgitations. In the two experiments, heart motion is recovered from gated short-axis cine-MRI. In the first experiment, the resulting 3D deformations are compared with tagged MRI. In the second experiment, the deformations are compared with ultra-sound 2D-strain.

Because we are mainly interested in myocardium strain and to minimise the computational overhead, diffeomorphic demons are constrained only inside a mask that delineates the cardiac muscle. As the projector Π and the elastic smoothing are decoupled from the minimisation, appearing as additive terms in the algorithm (Equations (3) and (4)), they can be added inside the mask and ignored outside (where diffeomorphic demons are still applied). It should be noted however that at the mask boundaries, the incompressibility constraint is not ensured due to the boundary conditions of the projector Π. Furthermore, discontinuities may appear at the mask boundaries when computing the displacement derivatives. These limitations are addressed by dilating the myocardium mask by one voxel, thus ensuring optimal strain estimation within the myocardium. At last, we need to segment the myocardium at the end-diastole time frame only owing to the Eulerian formulation of the demons algorithm, contrary to previous approaches which require delineations for all the cardiac sequence frames [3,5].

3.1 Left Ventricle Myocardium Strain in a Healthy Subject

Retrospective gated steady-state free precession (SSFP) cine MR and tagged MR (complementary spatial modulation of magnetisation CSPAMM) images of a healthy subject are acquired in the short-axis view covering the mid-part of both ventricles using 1.5T MR scanner (Achieva, Philips Medical System) (seven 10mm-thick slices; 1.37x1.37mm in-plane resolution, 30 frames). No longitudinal cine-MRI are available. Visual inspection of the images revealed no spatial misregistration. To improve registration performances, the resolution of the cine-MR images is made isotropic at the in-plane resolution.

First, the incompressibility constraint is evaluated by computing the Jacobian determinant of the recovered myocardium deformation at each frame of the cardiac sequence. Without any constraint, mean Jacobian equals 1.09 ± 0.07 (mean $\pm$ SD), maximum deviation from unity: 0.22. Adding the constraints yields $J(\mathbf{u}_{myo}) = 0.99 \pm 0.02$ (mean $\pm$ SD) with a maximum deviation from unity of 0.05, which relates to the observed 5% of myocardium volume variation [8].

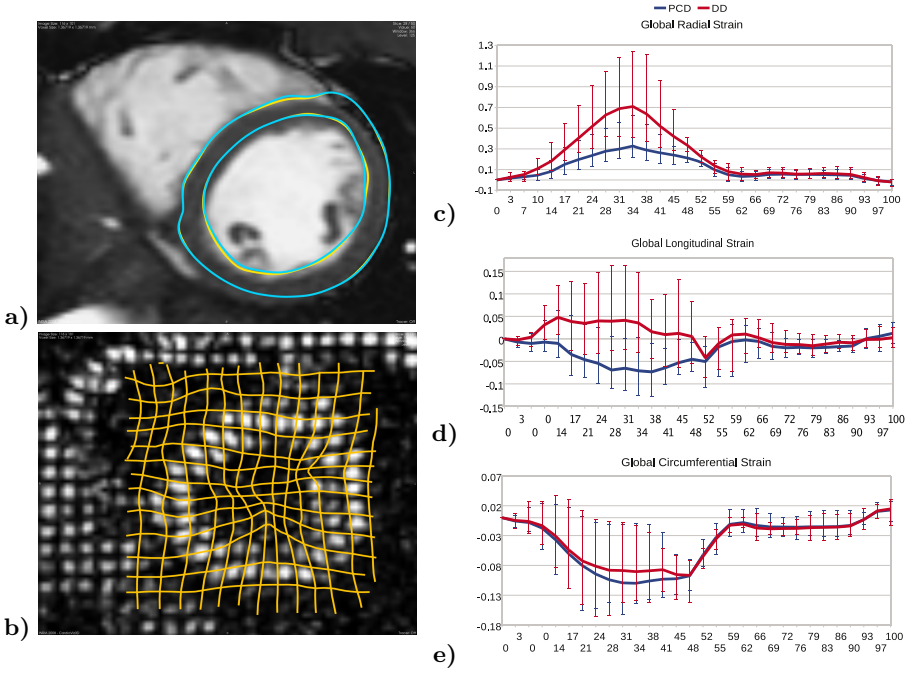

Fig. 1. a) End-systole myocardium mask propagated back to the end-diastole image using DD *(in yellow)* and PCD *(in blue)*. Both algorithms provide similar registration performances. b) Tagged-MRI at end-systole and tag grid deformed by the cine-MRI transformation estimated using PCD. c-e) Global strain with maximum and minimum zone values. Time is normalised in %.

Second, registered images provided by the physically-constrained demons (PCD) are compared with those provided by the diffeomorphic demons (DD). Available myocardium mask at end-systole is registered back to the end-diastole image using the two methods. Qualitative evaluation is satisfying (Fig. 1a). Hausdorff distance between the two registered masks is 2.23mm and average Hausdorff distance is 0.02mm, which is less than the through-plane image resolution. The physical constraints do not qualitatively decrease the registration performances.

Next, radial, longitudinal and circumferential strains are computed for the six equatorial AHA zones using DD and PCD. In this experiment, we only consider the equatorial zones since at the basal and apical regions the incompressibility assumptions may be violated due to the truncated acquisition. Fig. (1c-e) illustrate the global strains with minimum and maximum zone values. DD mainly recovers the visible radial motion of the heart, resulting in over-estimated radial strains, implausible positive longitudinal strains and weak circumferential strains. On the other hand, the physical constraints enable recovering non-apparent motions by reorienting the estimated myocardium deformations to ensure incompressibility. Radial strain is closer to clinical observations and more homogeneous across the myocardium [18], thus suggesting that the physical constraints also perform global regularisation. Longitudinal strain is clinically plausible yet slightly

under-estimated with respect to reported values, mainly because of the coarse through-plane resolution. Circumferential strain is improved but remains close to DD estimations. A probable reason is the low temporal resolution, circumferential motion occurring in few time frames.

Finally, the deformations recovered from the short-axis cine-MRI using PCD are qualitatively compared with short-axis tagged-MRI, exhibiting promising results (Fig. 1b).

3.2 Left-Ventricle Myocardium Strain in a Patient with Chronic Pulmonary Valve Regurgitations

In the second experiment we evaluate our method on a patient (age=10) with congenital pulmonary valve regurgitations. SSFP cine MRI of the heart are acquired in the short-axis view covering the entirety of both ventricles (10 9.6mm-thick slices; 1.02x1.02mm in-plane resolution; 25 frames) using a 1.5T MR scanner (Avanto, Siemens Medical Systems, Erlangen, Germany). No longitudinal cine-MRI are available. Visual inspection of the images revealed no spatial misregistration. Finally, the images are made isotropic to improve registration performances. 2D-strain measurements are performed in the short-axis and the 4-chamber views (frame-rate: 80) using Automatic Functional Imaging (Vivid7, General Electrics, Vingmed Ultrasound), as described in [2].

Lagrangian finite strain tensors are estimated from the cine-MRI. Longitudinal (L_l) and circumferential (L_c) lengthening are computed according to the relation $L_V = \sqrt{1 + \mathrm{E}_{VV}} + 1$, where E is the strain tensor and $V \in \{l, c\}$ is the

Table 1. Cine-MRI and 2D-strain (in parentheses) longitudinal lengthening. Values estimated from 3D MRI using PCD are close to the 2D measurements in spite of the different nature of the images.

Basal septal	Mid septal	Apical septal	Basal lateral	Mid lateral	Apical lateral
-0.11 (-0.19)	-0.18 (-0.19)	-0.19 (-0.09)	-0.10 (-0.11)	-0.12 (-0.11)	-0.07 (-0.11)

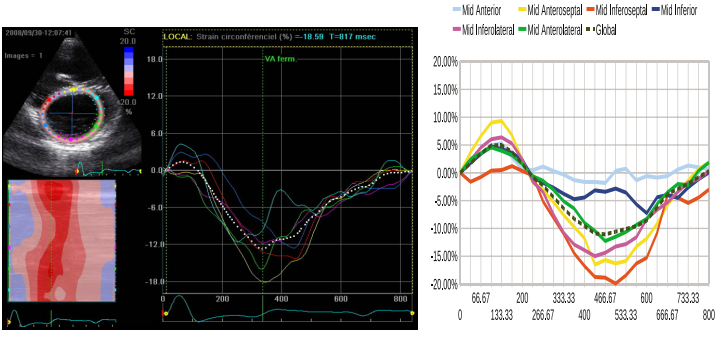

Fig. 2. Circumferential strain throughout the cardiac cycle. *Left*: 2D-strain measurement. *Right*: cine-MRI estimation. X-axis is the time in ms, Y-axis the strain in %.

considered direction. The results are compared with 2D-strain measurements. Despite of the different nature of the measurements, promising correlation is obtained. Estimated regional circumferential strains exhibit realistic variations (Fig. 2). Longitudinal strains are similar to the 2D-strain measurements in most of the heart regions visible in the acquired 2D slice (Table 1). However, as observed in the healthy subject, cine-MRI-derived longitudinal strains tend to be underestimated due to the large slice thickness. Finally, the apical septal strain has been overestimated because of the lower image quality at the apex and of the ill-defined left-right ventricles junction.

4 Conclusion

In this paper we demonstrate the effectiveness of a physically-constrained demons algorithm to recover cardiac motion from short-axis gated cine-MRI. Our approach improves the physical plausibility of the estimated myocardium deformations by constraining the registration algorithm to provide incompressible and elastic transformations. Incompressibility is modelled using divergence-free velocity fields, as defined by the mass-conservation law. A second correction is performed at the end of the demons loop to correct the positions from possible volume drifts resulting from the regularisation, which does not guarantee incompressibility. On the other hand, the second correction alone would not have been sufficient since it only approximates the strong volume-preserving constraint, thus yielding incomplete volume recovery. The physical constraints reorient the displacement vectors within the myocardium, which enables the recovery of longitudinal and circumferential motions. Compared with tagged-MRI and 2D-strain, the proposed method showed promising results for a healthy subject and a patient. Despite of the coarse longitudinal resolution, realistic through-plane motions have been recovered, yet under-estimated with respect to values reported in the literature. Future works include parameter-sensitivity study and comprehensive validation on controls and patients. This method may become a useful tool for cardiac function evaluation and retrospective studies.

Acknowledgements. The work has been partly funded by the European Commission through the IST-2004-027749 Health-e-Child Integrated Project[1]. The authors would like to thank Rado Andriantsimiavona, King's College London, Division of Imaging Sciences, for the cine and tagged MR images.

References

1. McVeigh, E.: Regional myocardial function. Cardiology Clinics 16(2), 189–206 (1998)
2. Teske, A., De Boeck, B., Melman, P., Sieswerda, G., Doevendans, P., Cramer, M.: Echocardiographic quantification of myocardial function using tissue deformation imaging, a guide to image acquisition and analysis using tissue doppler and speckle tracking. Cardiovascular Ultrasound 5, 27 (2007)

[1] http://www.health-e-child.org

3. Papademetris, X., Sinusas, A., Dione, D., Constable, R., Duncan, J.: Estimating 3D strain from 4D cine-MRI and echocardiography: In-vivo validation. In: Delp, S.L., DiGoia, A.M., Jaramaz, B. (eds.) MICCAI 2000. LNCS, vol. 1935, pp. 678–686. Springer, Heidelberg (2000)
4. Veress, A., Gullberg, G., Weiss, J.: Measurement of Strain in the Left Ventricle during Diastole with cine-MRI and Deformable Image Registration. Journal of Biomechanical Engineering 127, 1195 (2005)
5. Feng, W., Denney, T., Lloyd, S., Dell'Italia, L., Gupta, H.: Contour regularized left ventricular strain analysis from cine MRI. In: Proc. ISBI 2008, pp. 520–523 (2008)
6. Bistoquet, A., Oshinski, J., Skrinjar, O.: Myocardial deformation recovery from cine MRI using a nearly incompressible biventricular model. Medical Image Analysis 12(1), 69–85 (2008)
7. Delhay, B., Clarysse, P., Magnin, I.: Locally Adapted Spatio-temporal Deformation Model for Dense Motion Estimation in Periodic Cardiac Image Sequences. In: Sachse, F.B., Seemann, G. (eds.) FIMH 2007. LNCS, vol. 4466, p. 393. Springer, Heidelberg (2007)
8. Glass, L., Hunter, P., McCulloch, A.: Theory of Heart: Biomechanics, Biophysics, and Nonlinear Dynamics of Cardiac Function. Springer, Heidelberg (1991)
9. Vercauteren, T., Pennec, X., Perchant, A., Ayache, N.: Non-parametric diffeomorphic image registration with the demons algorithm. In: Ayache, N., Ourselin, S., Maeder, A. (eds.) MICCAI 2007, Part II. LNCS, vol. 4792, pp. 319–326. Springer, Heidelberg (2007)
10. Dupuis, P., Grenander, U., Miller, M.: Variational problems on flows of diffeomorphisms for image matching. Quaterly of Applied Mathematics 56(3), 587–600 (1998)
11. Ashburner, J.: A fast diffeomorphic image registration algorithm. Neuroimage 38(1), 95–113 (2007)
12. Rohlfing, T., Maurer Jr., C., Bluemke, D., Jacobs, M.: Volume-preserving nonrigid registration of MR breast images using free-form deformation with an incompressibility constraint. IEEE Transactions on Medical Imaging 22(6), 730–741 (2003)
13. Haber, E., Modersitzki, J.: Numerical methods for volume preserving image registration. Inverse Problems 20(5), 1621–1638 (2004)
14. Saddi, K.A., Chefd'hotel, C., Cheriet, F.: Large deformation registration of contrast-enhanced images with volume-preserving constraint. In: Proc. SPIE Medical Imaging, vol. 6512. SPIE (2007)
15. Simard, P.Y., Mailloux, G.E.: A projection operator for the restoration of divergence-free vector fields. IEEE Transactions on Pattern Analysis and Machine Intelligence 10(2), 248–256 (1988)
16. Modersitzki, J.: Numerical Methods for Image Registration. Oxford University Press, Oxford (2004)
17. Cachier, P., Ayache, N.: Isotropic energies, filters and splines for vectorial regularization. J. of Math. Imaging and Vision 20(3), 251–265 (2004)
18. Moore, C., Lugo-Olivieri, C., McVeigh, E., Zerhouni, E.: Three-dimensional systolic strain patterns in the normal human left ventricle: Characterization with tagged MR imaging. Radiology 214(2), 453–466 (2000)